Interactions of Amyloid β-Peptide (1−40) with Ganglioside-Containing Membranes†

Katsumi Matsuzaki* and Chiho Horikiri

Graduate School of Pharmaceutical Science, Kyoto University, Sakyo-ku, Kyoto 606-8501, Japan

Received September 30, 1998; Revised Manuscript Received January 20, 1999

ABSTRACT: Interactions between amyloid β-peptides (Aβ) and neuronal membranes have been postulated to play an important role in the neuropathology of Alzheimer's disease. To gain insight into the molecular details of this association, we investigated the interactions of Aβ (1−40) with ganglioside-containing membranes by circular dichroism (CD) and Fourier transform infrared-polarized attenuated total reflection (FTIR-PATR) spectroscopy. The CD study revealed that at physiological ionic strength Aβ (1−40) specifically binds to ganglioside-containing membranes inducing a two-state, unordered → β-sheet transition above a threshold intramembrane ganglioside concentration, which depends on the host lipid bilayers used. Furthermore, differences in the number and position of sialic acid residues of the carbohydrate backbone significantly affected the conformational transition of the peptide. FTIR-PATR spectroscopy experiments demonstrated that Aβ (1−40) forms an antiparallel β-sheet, the plane of which lies parallel to the membrane surface, inducing dehydration of lipid interfacial groups and perturbation of acyl chain orientation. These results suggest that Aβ (1−40) imposes negative curvature strain on ganglioside-containing lipid bilayers, disturbing the structure and function of the membranes.

Alzheimer's disease (AD)[1] is characterized by the presence of amyloid plaques surrounded by dead and dying neurons in the brain (*1*). The major component of the plaques is a 39−43-residue Aβ (*2*), a product of proteolytic processing of the much larger APP (*3*). A link between Aβ and AD neuropathological lesions is demonstrated by the toxicity of aggregated Aβ to neuronal cells in culture (*4*−*7*) and the aged brain (*8*). However, the molecular mechanisms of Aβ-induced neuronal cell death remain largely unknown.

A growing number of observations indicate that Aβ interacts with neuronal membranes disrupting ion homeostasis, therefore causing neurotoxicity although the molecular mechanisms of this interaction remain largely unknown. Aβ forms cation-selective ion channels in artificial phospholipid bilayers (*9*−*11*) as well as in neuronal membranes (*12*). The finding that all-D enantiomers of Aβ exhibit biological properties similar to those of native Aβ (*13*) suggests that Aβ neurotoxicity is mediated by physicochemical peptide−lipid interactions rather than stereospecific receptor−ligand interactions. The identification of a GM1-bound form of Aβ (*14*) stimulated interest in the interactions of Aβ with neuronal membranes which are rich in gangliosides (*15*). Aβ has been reported to bind to and permeabilize ganglioside-containing membranes (*16*−*19*), on which Aβ fibril formation is accelerated (*17*).

We report here the molecular aspects of interactions between Aβ (1−40) and ganglioside-containing membranes determined by use of CD and FTIR-PATR techniques. The peptide was found to bind to the bilayers in a two-state equilibrium, forming a β-sheet structure. The binding occurred only above a threshold molar fraction of ganglioside, which was highly dependent on the nature of the lipid matrix used. An increase in the number of sialic acid residues tended to enhance the interaction. The β-sheet was antiparallel and lay essentially on the membrane surface. The presence of the peptide induced dehydration of the lipid interfacial groups and slight disordering of acyl chains, suggesting that Aβ (1−40) imposes negative curvature strain on neuronal membranes, altering the bilayer organization and the functions of membrane proteins.

MATERIALS AND METHODS

Materials. Synthetic Aβ (1−40) was obtained from Peptide Institute Inc. (Osaka, Japan). The peptide was dissolved in HFIP and stored at −20 °C until use. Samples of the peptide for FTIR spectroscopy were lyophilized three times from 0.2 N HCl to replace the trifluoroacetate counterions with chloride. PG was a kind gift from Nippon Fine Chemical Co. (Takasago, Japan). PC, SM, Chol, GM1, GM3, and GT1b were purchased from Sigma (St. Louis, MO). GD1a and GD1b were obtained from Research Biochemicals International (Natick, MA). The bicinchoninic acid (BCA) protein assay kit was a product of Pierce (Rockford, IL). All other chemicals purchased from Wako (Tokyo, Japan) were of special grade.

Preparation of SUVs. A lipid film of the desired composition was dispersed in water or Tris buffer (10 mM Tris/150

† Supported in part by the Mochida Memorial Foundation for Medical and Pharmaceutical Research.

* To whom correspondence should be addressed. Telephone: 81-75-753-4574. Fax: 81-75-761-2698. E-mail: katsumim@pharm.kyoto-u.ac.jp.

[1] Abbreviations: Aβ, amyloid β-peptide; AD, Alzheimer's disease; APP, amyloid precursor protein; BCA, bicinchoninic acid; CD, circular dichroism; Chol, cholesterol; FTIR-PATR, Fourier transform infrared-polarized attenuated total reflection; GM1, monosialoganglioside GM1; GM3, monosialoganglioside GM3; GD1a, disialoganglioside GD1a; GD1b, disialoganglioside GD1b; GT1b, trisialoganglioside GT1b; HFIP, 1,1,1,3,3,3-hexafluoro-2-propanol; MLVs, multilamellar vesicles; PC, egg yolk L-α-phosphatidylcholine; PG, L-α-phosphatidylglycerol enzymatically converted from PC; SM, egg yolk sphingomyelin; SUVs, small unilamellar vesicles.

10.1021/bi982345o CCC: $18.00
Published on Web 03/09/1999

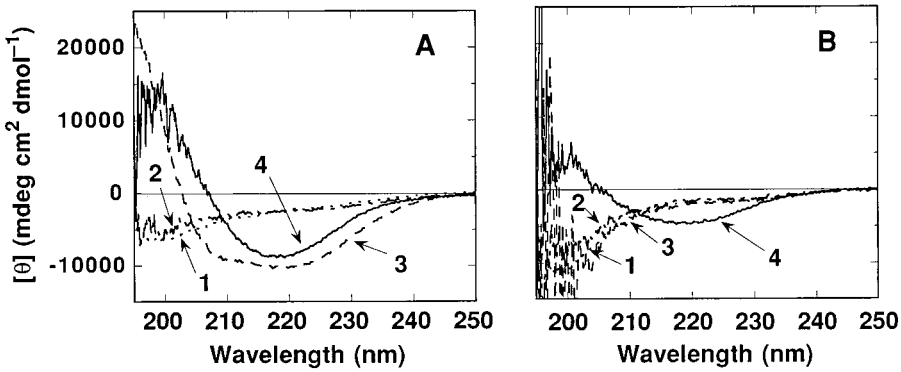

FIGURE 1: CD spectra of Aβ (1−40) (A) with no added salt and (B) in the presence of a physiological concentration of salt at 30 °C. (A) CD spectra of 1Aβ (1−40) in water were recorded in the absence (dotted trace 1) or presence of PC SUVs (dashed trace 2), PG SUVs (broken trace 3), or PG/GM1 (4/1) SUVs (solid trace 4). (B) CD spectra of Aβ (1−40) buffer solution were recorded in the absence (dotted trace 1) or presence of PC SUVs (dashed trace 2), PG SUVs (broken trace 3), or PG/GM1 (4/1) SUVs (solid trace 4). The peptide and lipid concentrations were 15 μM and 1.5 mM, respectively.

mM NaCl/1 mM EDTA, pH 7.4). The resulting MLVs were subjected to five freeze−thaw cycles and then sonicated in ice-cold water under a nitrogen atmosphere for 15 min by use of a probe-type sonicator. Metal debris from the titanium tip of the probe was removed by centrifugation.

CD Spectra. Aqueous peptide solutions for CD measurements were prepared by evaporating the organic solvent from stock peptide solution and redissolving the resulting peptide film in water or Tris buffer. CD spectra were measured on a Jasco J-720 apparatus interfaced to an NEC PC9801 microcomputer, using a 1 mm path-length quartz cell to minimize the absorbance due to buffer components. The instrumental outputs were calibrated with nonhygroscopic ammonium *d*-camphor-10-sulfonate. Eight scans were averaged for each sample. The averaged blank spectra (vesicle suspension or solvent) were subtracted. The peptide and the lipid concentrations were 15 μM and 0.75−1.5 mM, respectively.

FTIR-PATR Spectroscopy. Dry-cast films of PC/GM1 (4/1 mol/mol) or PC/GM1/Aβ (1−40) (40/10/1) were prepared by uniformly spreading an HFIP solution of PC (4.4 μmol)/GM1 (1.1 μmol) or PC (4.4 μmol)/GM1 (1.1 μmol)/Aβ (1−40) (0.11 μmol) on the surface of a germanium ATR plate (52 × 18 × 2 mm) followed by evaporation of the solvent. The film thickness estimated from the applied amount of the lipid was 5−6 μm. The lipid film was hydrated with pieces of D_2O-wet filter paper for 30 min to achieve complete hydration. Spectra were recorded on a Nicolet 205 FTIR spectrometer equipped with an Hg−Cd−Te detector. To minimize spectral contribution of atmospheric water vapor, the instrument was purged with N_2 gas. PATR measurements were carried out using a Perkin-Elmer multiple ATR attachment and a Specac KRS-5 polarizer. The angle of incidence was 45°, and the number of total reflections was 12 on the film side. The 256 interferograms collected had a resolution of 4 cm^{-1} and were analyzed by use of Nicolet SX software on a Nicolet 620 workstation. The subtraction of the gently sloping water vapor bands was carried out to improve the background prior to frequency measurement. The accuracy of the frequency reading was better than ± 0.1 cm^{-1}. The dichroic ratio, R, defined by $\Delta A_{\parallel}/\Delta A_{\perp}$, was calculated from the polarized spectra. The absorbance (ΔA) was obtained either as the peak height of each absorption band for the CH_2 symmetric stretching vibration or as the area of each component band for the deconvolved amide I′ bands. The subscripts $\parallel$ and $\perp$ refer to polarized light with its electric vector parallel and perpendicular to the plane of incidence, respectively. The baseline method was used to minimize the background artifact. Deconvolution and curve fitting of FTIR bands were performed by use of Nicolet FOCAS software. Deconvolution parameters of 25 cm^{-1} and 2.0 for the undeconvoluted band half-width and resolution enhancement factor, respectively, were used. Deconvoluted spectra were fitted with Gaussian band profiles.

All experiments (CD and FTIR) were carried out at least twice, and the results are expressed as averages ± SD.

RESULTS

CD Spectra. Conformations of Aβ (1−40) bound to membranes of various lipid compositions were estimated by use of CD. The spectra of a freshly prepared solution of Aβ (1−40) in both H_2O and the Tris buffer had a minimum at 197 nm, characteristic of a random coil conformation (Figure 1). Figure 1A shows that, in the absence of salt, the addition of electrically neutral PC vesicles induced no change in the CD spectrum, whereas in the presence of negatively charged PG vesicles, the spectrum exhibited double minima around 208 and 222 nm, characteristic of an α-helix. In contrast, GM1-containing vesicles [PC/GM1 (4/1)] induced a β-sheet conformation as suggested by a minimum at 218 nm.

In the Tris buffer of physiological ionic strength, addition of PG or PC vesicles to Aβ (1−40) resulted in no change in CD spectra (Figure 1B). On the other hand, Aβ (1−40) in the presence of GM1-containing membranes assumed a β-sheet conformation. The mean residue ellipticity at 218 nm is shown in Figure 2 as a function of intramembrane GM1 concentration. The conformational transition of Aβ (1−40) required a threshold value of GM1 concentration, which was dependent on the host lipid membranes used, i.e., 20 mol % in PG, 30 mol % in SM/Chol, and 40 mol % in PC. In addition, the spectra bound to the GM1-containing membranes exhibited an isodichroic point at 210 nm, providing evidence for a simple two-state random-β-structure equilibrium (Figure 3). However, the spectrum of Aβ (1−40) in the presence of micellar GM1 did not pass through the isodichroic point.

We also studied the conformation of Aβ (1−40) in the presence of GM3-, GD1a-, GD1b-, or GT1b-containing

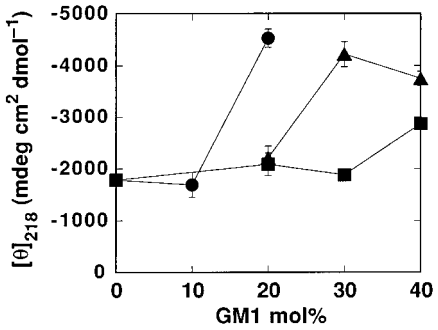

FIGURE 2: Threshold ganglioside concentrations required for Aβ binding. The mean residue ellipticity values at 218 nm of Aβ (1−40) in the presence of PC/GM1 (■), SM/Chol/GM1 (▲), or PG/GM1 (●) SUVs are plotted as a function of intramembrane GM1 concentration. The experimental conditions were the same as those in Figure 1. The GM1/peptide ratio was kept at 20.

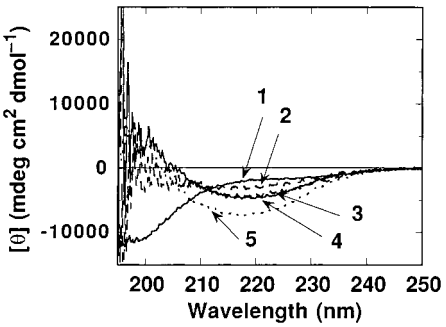

FIGURE 3: GM1-induced conformational changes in Aβ (1−40) at 30 °C. CD spectra of 15 μM Aβ (1−40) in Tris buffer were recorded in the absence (solid trace 1) or presence of SUVs composed of PC/GM1 (6/4) (broken trace 2), SM/Chol/GM1 (5/2/3) (broken trace 3), or PG/GM1 (8/2) SUVs (solid trace 4). Dotted trace 5 indicates the spectrum in the presence of GM1 micelles. The GM1/peptide ratio was kept at 20.

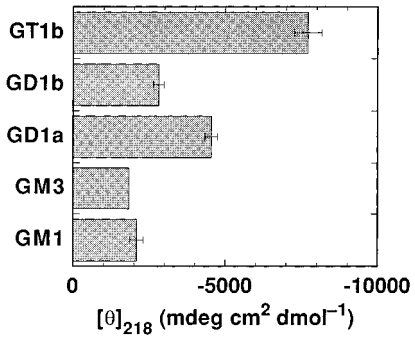

FIGURE 4: Effects of ganglioside species on Aβ binding. CD spectra of 15 μM Aβ (1−40) in Tris buffer in the presence of PC/ganglioside (4/1) SUVs at 30 °C were recorded at a ganglioside/Aβ molar ratio of 20. The mean residue ellipticity values at 218 nm are indicated as a measure of β-sheet formation.

vesicles. The results were similar to those of GM1-containing membranes. We observed CD spectra of β-type with a minimum at 218 nm and an isodichroic point at 210 nm (spectra not shown). As shown in Figure 4, differences in the number and position of sialic acid moieties in the carbohydrate backbone affected the structural transition of Aβ (1−40): the ability to induce a β-sheet was in the order GT1b > GD1a > GD1b > GM1 ≈ GM3.

Furthermore, we investigated the effects of Ca^{2+} on Aβ-ganglioside interactions because the extracellular aqueous phase contains ca. 1 mM Ca^{2+} and the divalent cation is known to weakly interact with gangliosides (*20*). CD spectra

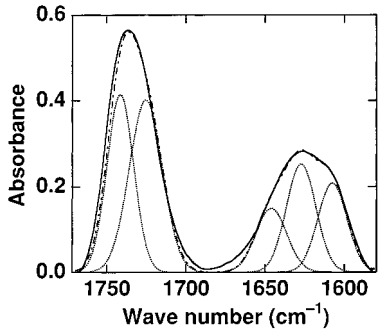

FIGURE 5: Unpolarized FTIR-ATR spectra of the D_2O-hydrated film of PC/GM1 (4/1). The solid trace denotes the observed spectrum. The dotted traces represent the component band contours obtained from the Fourier self-deconvolution and curve-fitting procedure. The dashed trace represents the sum of the resolved bands.

of Aβ (1−40) were recorded in the presence of ganglioside-containing vesicles dispersed in the Tris buffer containing 1 mM $CaCl_2$ (EDTA was omitted). However, the presence of Ca^{2+} did not affect the ability of gangliosides to induce formation of a β-sheet (data not shown).

FTIR-PATR. FTIR spectroscopy is useful for investigating peptide−lipid interactions because the conformations of functional groups of both peptides and lipids can be simultaneously estimated without perturbation (*21*−*24*). The PATR technique enabled us to evaluate molecular orientation (*23*, *25*−*27*). Figure 5 shows unpolarized ATR spectra of D_2O-hydrated PC/GM1 (4/1) films in the region 1600−1800 cm^{-1}, which were calculated as a linear combination of polarized spectra (*26*). Deconvolution and curve fitting resolved the observed spectra (solid trace) into five component bands. The band at 1605 cm^{-1} can be assigned to the carboxylate antisymmetric stretching (*28*, *29*). The bands at 1626 and 1645 cm^{-1} corresponded to fully hydrated and less hydrated amide I′ groups (*29*), respectively. The bands at 1741 and 1725 cm^{-1} originated from non-hydrogen-bonded and hydrogen-bonded carbonyl groups, respectively (*30*).

Figure 6A shows unpolarized ATR spectra of D_2O-hydrated PC/GM1/Aβ (1−40) (40/10/1) films in the region of 1600−1800 cm^{-1}. The amide I′ band could be resolved into five component bands centered at 1605, 1626, 1646, 1665, and 1693 cm^{-1}. The band at 1605 cm^{-1} originated from the COO^- antisymmetric stretching. If we assume that the band at 1646 cm^{-1} was solely attributable to the GM1 amide group (vide infra), most (84%) of the intensity of the strongest 1626 cm^{-1} band should come from the Aβ amide group, because the carbonyl-to-amide I′ intensity ratio of GM1 (2.0 obtained from Figure 5) should be conserved irrespective of the presence of Aβ (1−40). Therefore, the combined bands at 1626 and 1693 cm^{-1} were assigned to an antiparallel β-sheet conformation (*31*). The former absorption corresponded to the $\nu(\pi, 0)$ transition and the latter to the $\nu(0, \pi)$ transition. The band at 1665 cm^{-1} can be assigned to turn structures (*32*). The β-sheet content of Aβ (1−40) was estimated to be 80% [$100(0.84\Delta A_{1626} + \Delta A_{1693})/(0.84\Delta A_{1626} + \Delta A_{1665} + \Delta A_{1693})$]. The conformation of the peptide is that of the membrane-bound form because the peptide binding was complete under these experimental conditions, as confirmed below. A PC/GM1/Aβ (1−40) (40/10/1) film was hydrated with H_2O at a PC concentration of 1 mM and vortex-mixed. The resulting MLV suspension was

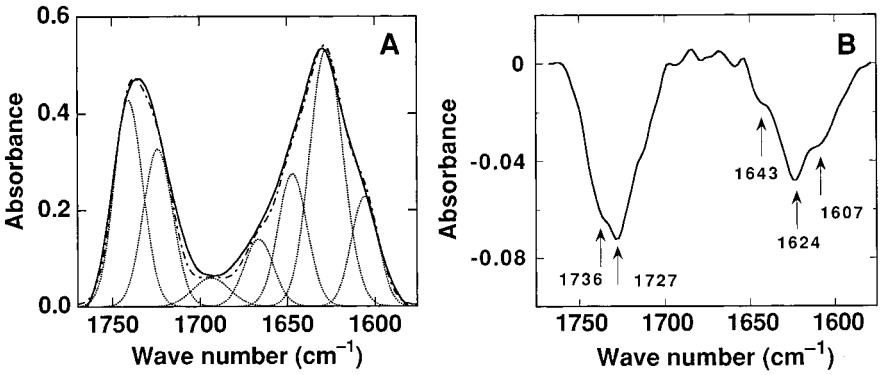

FIGURE 6: FTIR-ATR spectra of the D_2O-hydrated film of PC/GM1/Aβ (40/10/1). (A) Unpolarized spectra. The solid trace denotes the observed spectrum. The dotted traces represent the component band contours obtained from the Fourier self-deconvolution and curve fitting procedure. The dashed trace represents the sum of the resolved bands. (B) Dichroic spectrum, $\Delta A_{\parallel} - 2\Delta A_{\perp}$.

Table 1: Conformations and Orientations of Lipid Hydrocarbon Chains

sample[a]	wavenumber (cm^{-1})[b]	$R^{b,c}$	S^d	α (deg)[e]
PC	2852.5 ± 0.4	1.33 ± 0.01	0.49 ± 0.01	35.8 ± 0.3
PC/Aβ (1−40)	2853.3 ± 0.1	1.39 ± 0.05	0.43 ± 0.04	37.9 ± 1.7
PC/GM1	2851.5 ± 0.1	1.28 ± 0.04	0.53 ± 0.04	34.1 ± 1.6
PC/GM1/Aβ (1−40)	2851.3 ± 0.2	1.49 ± 0.01	0.35 ± 0.01	41.3 ± 0.4

[a] Samples were hydrated with D_2O. The lipid/peptide molar ratio was 50. The PC/GM1 molar ratio was 4. [b] CH_2 symmetric stretching band. [c] Dichroic ratio. [d] Order parameter of the acyl chain. [e] Mean orientational angle between the hydrocarbon chain and the membrane normal.

ultracentrifuged at 150000*g* for 1 h for the separation of free and membrane-bound peptides. The peptide concentration of the supernatant determined by the BCA assay was only 2% of the total peptide concentration. Therefore, all peptides were membrane-bound in the FTIR experiments, where the local lipid concentration was much higher. In contrast, in the absence of GM1 [PC/Aβ (1−40) = 40/1], most (>70%) of the peptide was recovered from the supernatant.

The addition of Aβ (1−40) caused dehydration of lipid backbone groups. The relative contributions of the bands at 1646 and 1741 cm^{-1} to the amide I′ and carbonyl stretching bands increased from 38% to 74% and from 45% to 56%, respectively.

The dichroic ratio, *R*, of an absorption band obtained by PATR spectra is a measure of the orientation of its transition moment or molecular axis. For membranes much thicker (∼6 μm) than the penetration depth (under our experimental conditions, 0.2−0.8 μm in the range 3000−800 cm^{-1}), an *R* value smaller than 2 indicates that the moment lies essentially parallel to the membrane surface (*23*, *25*, *26*). Figure 6B shows the dichroic spectrum, $\Delta A_{\parallel} - 2\Delta A_{\perp}$, which does not contain contributions from isotropic signals, if any. Negative peaks and shoulders were found at 1607, 1624, 1643, 1727, and 1736 cm^{-1}, which correspond to the major bands resolved in Figure 6A. Small shifts in wavenumber are due to spectral overlap. Thus, the transition moments of these bands are oriented essentially parallel to the Ge plate. If the band at 1646 cm^{-1} had originated from a random structure of the peptide, such an orientation would not have been observed. Quantitative estimation of the orientation of the β-sheet was based on *R* values. Both the $\nu(\pi, 0)$ and the $\nu(0, \pi)$ transition moments, which are in the plane of the β-sheet (*31*), lay parallel to the membrane surface, because the *R* values were 1.71 ± 0.01 and 1.13 ± 0.02, respectively. The contribution of the GM1 amide I′ band to the 1626 cm^{-1} component had been subtracted, assuming that the orientation of the group did not change upon interaction with the peptide, although this correction was small.

Table 2: Wavenumber of Lipid Polar Group Vibrations

sample[a]	wavenumber (cm^{-1}) $\nu_{as}[N^+(CH_3)_3]$	$\nu_s(PO_2^-)$	$\nu_{as}(COO^-)$
PC/GM1	972.1 ± 0.2	1085.8 ± 0.1	1606.3 ± 0.5
PC/GM1/Aβ (1−40)	972.2 ± 0.2	1086.6 ± 0.9	1604.8 ± 0.4

[a] Samples were hydrated with D_2O. The lipid/peptide molar ratio was 50. The PC/GM1 molar ratio was 4.

Peptide-induced perturbation of bilayer structures was estimated by examining the CH_2 symmetric stretching band near 2850 cm^{-1}. Table 1 summarizes the frequency and order parameter, *S*, of the lipid hydrocarbon chain calculated from the dichroic ratio by use of eq 1 (*25*−*27*). This parameter is

$$S = -2(R - 2)/(R + 1.45) \quad (1)$$

connected to the mean orientation angle, α, between the hydrocarbon chain and the membrane normal through eq 2,

$$S = (1/2)(3\cos^2\alpha - 1) \quad (2)$$

assuming the uniaxial orientation of the chain around the normal. The order parameter for D_2O-hydrated PC films was little affected by the addition of Aβ (1−40). In contrast, the presence of Aβ (1−40) in D_2O-hydrated PC/GM1 films significantly reduced the order parameter, indicating that the orientation axis of the lipid was perturbed by the peptide.

Table 2 summarizes the effects of Aβ (1−40) on the peak frequencies of lipid polar group vibrations. Upon association of Aβ (1−40) with PC/GM1 membranes, the frequencies of the PO_2^- symmetric stretching band or the $N^+(CH_3)_3$ antisymmetric stretching band were not affected, whereas the COO^- antisymmetric stretching vibration was shifted by 1.5 cm^{-1} to lower wavenumbers.

DISCUSSION

CD Spectra. Aβ (1−40) assumes an unordered structure in aqueous solution (Figure 1), indicating that the peptide is not fibrillated. The absence of fibrillation was also confirmed by the thioflavin T assay (*33*) (data not shown). In the absence of salt (Figure 1A), Aβ (1−40) selectively binds to negatively charged membranes forming either an α-helix (PG) or a β-sheet (PC/GM1). Terzi et al. (*34*) reported that the peptide undergoes an α-helix → β-sheet transition on PG bilayers at L/P <55. In contrast, at physiological ionic strength, where electrostatic interactions are weakened, Aβ−PG interactions were lost (Figure 1B), in agreement with previous studies (*16*, *18*, *35*), whereas Aβ (1−40) can still recognize gangliosides, forming a β-sheet (Figures 1B and 3). McLaurin et al. (*16*, *19*) reported that the peptide forms an α- helix rather than a β-structure upon association with gangliosides at pH 7. The reason for this discrepancy may be differences in sample preparation. They added Aβ (1−40) dissolved in a trifluoroethanol/water mixture to lipid vesicles. On the other hand, we prepared an organic solvent-free aqueous solution of Aβ (1−40) which had been stored in HFIP, a solvent that prevents peptide aggregation (*36*). The initial solution state has been reported to markedly affect ion channel properties of Aβ (*37*).

We have shown that the binding of Aβ (1−40) to ganglioside-containing membranes requires a threshold value for intramembrane ganglioside concentration (Figure 2), suggesting that the peptide recognizes a ganglioside-rich domain (*38*, *39*), the formation of which depends on the host lipid membrane. Compared with PC, the threshold value was smaller in SM/Chol membranes, which mimics a detergent-insoluble glycolipid-enriched membrane domain containing Aβ in vivo (*40*). The low threshold value (10%) in PG bilayers may be explained by the electrostatic concentration of Aβ near the negatively charged membrane surface (*35*).

CD spectra of Aβ (1−40) in the presence of ganglioside-containing bilayers exhibited the isodichroic point, but CD spectra in the presence of micellar GM1 did not pass this point (Figure 3). Moreover, differences in the number and position of sialic acid residues of gangliosides affected the structural transition of the peptide (Figure 4). These observations suggested that Aβ (1−40) can recognize detailed conformations and orientations of the ganglioside headgroups.

FTIR-PATR. CD spectroscopy is not suitable for quantitative estimation of nonhelical secondary structures (*41*). FTIR spectra clearly indicated that Aβ (1−40) essentially forms an antiparallel β-sheet structure (∼80%). On the other hand, a theoretical study predicted that the peptide adopts a secondary structure composed of 55% helix and 20% antiparallel β-sheet in phosphatidylserine bilayers (*42*). The peptide might undergo a β-sheet → α-helix transition depending on the lipid-to-peptide ratio (*34*). However, this was not the case at least at GM1/Aβ (1−40) ratios of 20−200 (Figures 1 and 6).

Estimation of the sheet plane orientation requires the dichroic ratio of both the intense $\nu(\pi, 0)$ band at 1626 cm^{-1} and the weak $\nu(0, \pi)$ band at 1693 cm^{-1}, the transition moments of which lie in the sheet plane and are perpendicular to each other (*31*). The angles between these transition moments and the bilayer normal are denoted by *a* and *b*, respectively. Assuming the uniaxial orientation of each transition moment around the bilayer normal (*26*), the order parameter, S_a or S_b, defined by equations similar to eq 2, can be estimated by eq 3 (*27*). The order parameter of the

$$S_a \text{ (or } S_b) = (R - 2)/(R + 1.45) \quad (3)$$

sheet normal, S_c, can be evaluated by use of eq 4 (*27*). The

$$S_a + S_b + S_c = 0 \quad (4)$$

calculated S_c value was 0.44 ± 0.02, which corresponds to an orientation angle of 38°, although this estimate may contain some errors because of the weak overlapping features of both $\nu(\pi, 0)$ and $\nu(0, \pi)$ bands. This theoretical treatment was essentially the same as that recently reported by Marsh (*43*). The positive S_c value implies that the sheet normal is essentially perpendicular to the plane of the Ge plate. Further, our S_c value was in good agreement with the order parameters of the lipid hydrocarbon chain, *S* (Table 1). Thus, we concluded that the Aβ (1−40) antiparallel β-sheet lies parallel to the membrane surface.

Table 2 clearly shows that Aβ (1−40) does not strongly interact with the polar headgroups of PC, compatible with the observation that the peptide does not bind to PC bilayers (Figure 1). In contrast, the presence of Aβ (1−40) shifted the COO^- antisymmetric stretching band to lower frequencies, suggesting that the peptide hydrogen-bonds to the carboxylate group. The crucial role of the sialic acid moiety in Aβ−ganglioside interactions has been reported (*16*, *18*). This conclusion is further strengthened by the observation that gangliosides with larger numbers of sialic acid residues bind Aβ (1−40) more strongly (Figure 4).

The binding of Aβ (1−40) causes dehydration of the backbone groups of both GM1 and PC, although the recognition site appears to be the sialic acid moiety. Furthermore, the acyl chain orientation is perturbed by peptide binding. These observations are compatible with the hypothesis that Aβ (1−40) imposes negative curvature strain on the membrane, although the polar headgroup of PC is not significantly affected by the peptide (Table 2). In other words, the peptide counteracts gangliosides, which generate domains of high curvature in membranes (*44*). Aβ-induced permeabilization of ganglioside-containing membranes (*16*, *19*) may be related to the peptide-induced perturbation of bilayer organization.

In conclusion, the CD and FTIR-PATR experiments revealed that Aβ (1−40) recognizes domains of gangliosides, forms an antiparallel β-sheet lying parallel to the lipid bilayer, and imposes negative curvature strain on lipid membranes.

Gangliosides are abundant components of neuronal membranes. Functionally, they have been implicated in a number of important neurobiological events such as neurodifferentiation, neuritogenesis, synaptogenesis, and synaptic transmission. The interactions between Aβ (1−40) and gangliosides seem to play an important role in Aβ-induced neuronal degeneration. The arrest of gangliosides by Aβ would affect their metabolism. Aβ permeabilizes ganglioside-containing membranes and thus disturbs ion homeostasis (*16*, *19*). The local concentration of the peptide on the membrane surface can facilitate the formation of toxic aggregates. Furthermore, a great deal of attention has been paid to the role of hydration

in the functioning of various membrane proteins, such as protein kinase C (*45*). Changes in physical properties of neuronal membranes can affect intracellular signaling.

REFERENCES

1. Selkoe, D. J. (1991) *Neuron 6*, 487−498.
2. Glenner, G. G. (1984) *Biochem. Biophys. Res. Commun. 120*, 885−890.
3. Kang, J., Lemaire, H.-G., Unterbeck, A., Salbaum, J. M., Masters, C. L., Grzeschik, K.-H., Multhaup, G., Beyreuther, K., and Müller-Hill, B. (1987) *Nature 325*, 733−736.
4. Yankner, B. A., Duffy, L. K., and Kirschner, D. A. (1990) *Science 250*, 279−282.
5. Pike, C. J., Walencewicz, A. J., Glabe, C. G., and Cotman, C. W. (1991) *Brain Res. 563*, 311−314.
6. Ueda, K., Fukui, Y., and Kageyama, H. (1994) *Brain Res. 639*, 240−244.
7. Lambert, M. P., Barlow, A. K., Chromy, B. A., Edwards, C., Freed, R., Liosatos, M., Morgan, T. E., Rozovsky, I., Trommer, B., Viola, K. L., Wals, P., Zhang, C., Finch, C. E., Krafft, G. A., and Klein, W. L. (1998) *Proc. Natl. Acad. Sci. U.S.A. 95*, 6448−6453.
8. Geula, C., Wu, C.-K., Saroff, D., Lorenzo, A., Yuan, M., and Yankner, B. A. (1998) *Nat. Med. 4*, 827−831.
9. Arispe, N., Rojas, E., and Pollard, H. B. (1993) *Proc. Natl. Acad. Sci. U.S.A. 90*, 567−571.
10. Arispe, N., Pollard, H. B., and Rojas, E. (1993) *Proc. Natl. Acad. Sci. U.S.A. 90*, 10573−10577.
11. Rhee, S. K., Quist, A. P., and Lal, R. (1998) *J. Biol. Chem. 273*, 13379−13382.
12. Kawahara, M., Arispe, N., Kuroda, Y., and Rojas, E. (1997) *Biophys. J. 73*, 67−75.
13. Cribbs, D. H., Pike, C. J., Weinstein, S. L., Velazquez, P., and Cotman, C. W. (1997) *J. Biol. Chem. 272*, 7431−7436.
14. Yanagisawa, K., Odaka, A., Suzuki, N., and Ihara, Y. (1995) *Nat. Med. 1*, 1062−1066.
15. Schwarz, A., and Futerman, A. H. (1996) *Biochim. Biophys. Acta 1286*, 247−267.
16. McLaurin, J., and Chakrabartty, A. (1996) *J. Biol. Chem. 271*, 26482−26489.
17. Choo-Smith, L.-P., Garzon-Rodriguez, W., Glabe, C. G., and Surewicz, W. K. (1997) *J. Biol. Chem. 272*, 22987−22990.
18. Choo-Smith, L.-P., and Surewicz, W. K. (1997) *FEBS Lett. 402*, 95−98.
19. McLaurin, J., Franklin, T., Fraser, P. E., and Chakrabartty, A. (1998) *J. Biol. Chem. 273*, 4506−4515.
20. McDaniel, R., and McLaughlin, S. (1985) *Biochim. Biophys. Acta 819*, 153−160.
21. Amey, R. L., and Chapman, D. (1984) in *Biomembrane Structure and Function* (Chapman, D., Ed.) pp 199−256, Verlag Chemie, Weinheim.
22. Casal, H. L., and Mantsch, H. H. (1984) *Biochim. Biophys. Acta 779*, 381−401.
23. Haris, P. I., and Chapman, D. (1996) in *Infrared Spectroscopy of Biomolecules* (Mantsch, H. H., and Chapman, D., Eds.) pp 239−278, Wiley-Liss, New York.
24. Tamm, L., and Tatulian, S. A. (1997) *Q. Rev. Biophys. 30*, 365−429.
25. Okamura, E., Umemura, J., and Takenaka, T. (1986) *Biochim. Biophys. Acta 856*, 68−75.
26. Matsuzaki, K., Shioyama, T., Okamura, E., Umemura, J., Takenaka, T., Takaishi, Y., Fujita, T., and Miyajima, K. (1991) *Biochim. Biophys. Acta 1070*, 419−428.
27. Matsuzaki, K., Nakayama, M., Fukui, M., Otaka, A., Funakoshi, S., Fujii, N., Bessho, K., and Miyajima, K. (1993) *Biochemistry 32*, 11704−11710.
28. Müller, E., Giehl, A., and Blume, A. (1993) *Biochim. Biophys. Acta 1146*, 45−51.
29. Müller, E., Giehl, A., Schwarzmann, G., Sandhoff, K., and Blume, A. (1996) *Biophys. J. 71*, 1400−1421.
30. Blume, A., Hübner, W., and Messner, G. (1988) *Biochemistry 27*, 8239−8249.
31. Miyazawa, T. (1960) *J. Chem. Phys. 32*, 1647−1652.
32. Vandenbussche, G., Clercx, A. Clercx, M., Curstedt, T., Lohansson, J., Jörnvall, H., and Ruysschaert, J.-M. (1992) *Biochemistry 31*, 9169−9176.
33. Levine, H., III (1993) *Protein Sci. 2*, 404−410.
34. Terzi, E., Hölzemann, G., and Seelig, J. (1997) *Biochemistry 36*, 14845−14852.
35. Terzi, E., Hölzemann, G., and Seelig, J. (1995) *J. Mol. Biol. 252*, 633−642.
36. Snyder, S. W., Ladror, U. S., Wade, W. S., Wang, G. T., Barrett, L. W., Matayoshi, E. D., Huffaker, H. J., Krafft, G. A., and Holzman, T. F. (1994) *Biophys. J. 67*, 1216−1228.
37. Hirakura, Y., Kirino, Y., and Kagan, B. L. (1998) *Biophys. J. 74*, A389.
38. Ferraretto, A., Pitto, M., Palestini, P., and Masserini, M. (1997) *Biochemistry 36*, 9232−9236.
39. Brown, D. A., and Rose, J. K. (1992) *Cell 68*, 533−544.
40. Lee, S.-J., Liyanage, U., Bickel, P. E., Xia, W., Lansbury, P. T., Jr., and Kosik, K. S. (1998) *Nat. Med. 4*, 730−734.
41. Yang, J. T., Wu, C.-S. C., and Martinez, H. M. (1986) *Methods Enzymol. 130*, 208−269.
42. Durell, S. R., Guy, H. R., Arispe, N., Rojas, E., and Pollard, H. B. (1994) *Biophys. J. 67*, 2137−2145.
43. Marsh, D. (1997) *Biophys. J. 72*, 2710−2718.
44. Van Gorkom, L. C. M., Cheetham, J. J., and Epand, R. M. (1995) *Chem. Phys. Lipids 76*, 103−108.
45. Giorgione, J. R., and Epand, R. M. (1997) *Biochemistry 36*, 2250−2256.

BI982345O